

# 3-D Security Checkpoints Imaging Using W-K Algorithm

<sup>I</sup>Feng He, <sup>II</sup>Yi Chen, <sup>III</sup>Qingliang Cao, <sup>IV</sup>Yi Ren

<sup>I</sup>College of Optoelectronic Engineering, Chongqing University of Posts and  
Telecommunications, Chongqing 400065, China

<sup>II,III,IV</sup>College of Communication and Information Engineering, Chongqing University of  
Posts and Telecommunications, Chongqing 400065, China

## Abstract

Millimeter wave (MMW) imaging technology has using three-dimensional W-K (also called Range Migration Algorithm, RMA) to reconstruct a focused image of the concealed object through its reflect waves, and this technology is well suited for the detection of concealed weapons or contraband carried by personnel in airports or other places of safety. In this paper, a wavenumber domain algorithm with motion compensation is presented, which also use the stolt interpolation to obtain uniform wavenumber samples and compute the Fast Fourier Transform (FFT). The MMW security checkpoints system utilizes a 32.5-37.5 GHz linear sequentially scanner to scan targets. Numerical simulations and experimental results have demonstrated the algorithm has high computational efficiency and accurate image reconstruction.

## Keywords

Three-dimensional RMA, millimeter wave imaging, concealed weapons, linear scanner, wavenumber domain.

## I. Introduction

Recently, security checkpoints has attracted much attention. Many public places like airports, customs, railway stations etc. Have a high demand for the accuracy, real-time capability and intelligentize of the security system. However it is still difficulties to check out something that hidden in human body, Traditional security testing equipment (Metal Detection, X-ray imaging equipment) have many defects<sup>[8]</sup>.

Metal detectors can inspect knives, guns and other fobidden metal objects that someone takes, but it can't detect modern dangerous items like ceramic tool and liquid explosives; X-ray imaging equipment are ionizing, so it is unfit for personnel security check<sup>[1]</sup>.

From methods mentioned above, the traditional security checkpoints equipment are not suitable for public. In this paper, we use the method of active millimeter-wave security checkpoints imaging. Millimeter-wave holographic imaging for concealed weapon detection was originally proposed by Farhat and Guard<sup>[10]</sup>. The reason why we choose this method is millimeter-wave has the features of penetrativity and nonionizing which can be used for security checkpoints. Since passive imaging system cannot complete 3-D imaging so we instead choose the active method, by which the security checkpoints imaging system emits millimeter, then detect the backscatter data to apply w-k algorithm (also called Range Migration Algorithm, RMA) to reconstruction the image of the be tested object.

## II. 3-D RMA

Because of security checkpoints imaging is near-field, the distance only can lead to phase change, it doesn't influence on the range so we consider using RMA Which is a wavefront inversion method and originates from seismics engineering and geophysics<sup>[1]</sup>. 3-D RMA is an extension of the 2-D range migration algorithm (RMA). The RMA algorithm, as all SAR algorithm, is based on a linearization of the electromagnetic wave scattering problem. So it requires a one-dimensional (1-D) interpolation (known as stolt interpolation) to compensates completely the curvature of the wavefront, no matter it's 2-D or 3-D RMA.

Assuming that 2-D synthetic aperture is planar and within the near-field zone of the target. Frequency domain backscatter data can be obtained by using a stepped frequency radar which is required

by the algorithm<sup>[2]</sup>. The frequency-domain data is preferred because the RMA realizes the reconstruction of the target image in frequency wavenumber domain.

The measurement configuration of Planar aperture 3-D imaging is shown in Fig. 1. The source is assumed to be at the position  $(x_a, -R_0, z_a)$ , the distance  $R_0$  between antenna element and target plane. Scan stepped  $\Delta x_a$  and  $\Delta z_a$  in the horizontal and vertical cross-range directions, respectively. The two-way frequency wavenumber is directly associated with frequency,  $f = ck_r/2\pi$   $c$  is the speed of light. A general point on the target is assumed to be at the position  $(x, y, z)$  and the reflectivity function  $\sigma(x, y, z)$ , then the acquired backscatter data is  $d(x_a, k_r, z_a)$ <sup>[3]</sup>.

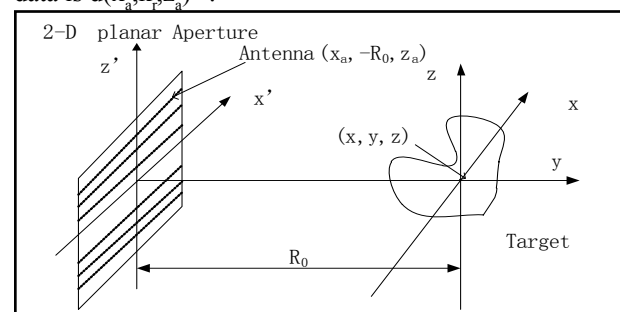


Fig.1 : Measurement and imaging geometry

$$d(x_a, k_r, z_a) = \sigma(x, y, z) \exp[j2k_r R_0] \exp[-j2k_r R] \quad (1)$$

Where  $R$  is the range to the point scatters, i.e.,

$$R = \sqrt{(x_a - x)^2 + (-R_0 - y)^2 + (z_a - z)^2} \quad (2)$$

For the convenience of next calculation, we can not consider the losses due to free-space propagation and the antenna pattern. 2-D horizontal and vertical cross-range FFT of the frequency-domain backscatter data is  $D(k_x, k_r, k_z)$ ,

$$D(k_x, k_r, k_z) = \iint \sigma(x, y, z) \exp[j2k_r R_0] \exp[-j2k_r R] \exp[-jk_x x_a - jk_z z_a] dx_a dz_a \quad (3)$$

Assuming the integrals in equation (3),

$$E(k_x, k_z) = \iint \exp[-j2k_r R] \exp[-jk_x x_a - jk_z z_a] dx_a dz_a \quad (4)$$

so it can be evaluated analytically by using the method of stationary phase (MSP)<sup>[4]</sup>. The phase of the exponential is given by  $\Phi(x, z) = -2k_r R - k_x x_a - k_z z_a$ . The stationary point  $(x_0, z_0)$  is an extreme value of the phase  $\Phi(x, z)$  i.e.,

$$\frac{\partial \Phi}{\partial x_a} \Big|_{(x_a = x_0)} = 0 \quad (5)$$

$$\frac{\partial \Phi}{\partial z_a} \Big|_{(z_a = z_0)} = 0 \quad (6)$$

According to equation (5)(6), the stationary point  $(x_0, z_0)$  is

$$x_0 = -\frac{k_x(y + R_0)}{\sqrt{4k_r^2 - k_x^2 - k_z^2}} + x \quad (7)$$

$$z_0 = -\frac{k_z(y + R_0)}{\sqrt{4k_r^2 - k_x^2 - k_z^2}} + z \quad (8)$$

Then 2-D integrals in (4) by means of the method of stationary phase (MSP) result in:

$$E(k_x, k_r) \Big|_{(x_0, z_0)} \approx \exp(-j\sqrt{4k_r^2 - k_x^2 - k_z^2}(y + R_0)) \times \exp(-jk_x x - jk_z z) \quad (9)$$

Take the equation (9) into equation (3),

then the acquired backscatter data is  $d(x_a, k_r, z_a)$ <sup>[3]</sup>.

$$D(k_x, k_r, k_z) = \sigma(x, y, z) \times \exp(-j\sqrt{4k_r^2 - k_x^2 - k_z^2} R_0) \times \exp(-jk_x x - jk_z z - j\sqrt{4k_r^2 - k_x^2 - k_z^2} y) \times \exp(j2k_r R_0) \quad (10)$$

From (1), the 3-D reflectivity can be expressed as

$$\sigma(x, y, z) = \int \exp[-j2k_r R_0] \iint d(x_a, k_r, z_a) \cdots \times \exp[j2k_r \sqrt{(x_a - x)^2 + (-R_0 - y)^2 + (z_a - z)^2}] dx_a dz_a dk_r \quad (11)$$

the 3-D reflectivity image is given by

$$\sigma(x, y, z) \approx \iiint D(k_x, k_r, k_z) \cdots \times \exp[j(k_x x + k_z z + \sqrt{4k_r^2 - k_x^2 - k_z^2}(y + R_0))] \times \exp(-j2k_r R_0) dk_x dk_r dk_z \quad (12)$$

Where  $k_y = \sqrt{4k_r^2 - k_x^2 - k_z^2}$  is uniform distribution. The spatial

wavenumber  $k_x$  and  $k_z$  are the Fourier-transform variable corresponding to  $x$  and  $y$ , respectively. Meanwhile,  $k_x$  and  $k_z$  will range from  $-2k$  to  $2k$  for propagating waves<sup>[6]</sup>. However, before last step (3-D IFFT) of algorithm, the wavenumber backscatter data  $k_r$  must be resampled by uniformly in  $k_y$ . This is the key to 3-D inverse FFT. The 3-D reflectivity image takes the form

$$\sigma(x, y, z) \approx \iiint D(k_x, k_y, k_z) \exp[jk_x x + jk_z z + jk_y y] \exp(-j2k_r R_0 + jk_y R_0) dk_x dk_y dk_z \quad (13)$$

Combining the above relations, the image reconstruction can be given by

$$\sigma(x, y, z) = IFFT_{(k_x, k_y, k_z)} [D(k_x, k_y, k_z) e^{-j2k_r R_0 + jk_y R_0}] \quad (14)$$

The image reconstruction process consists of the following steps in Fig.2:

The frequency domain data is equal to the test data subtract the background data, then do 2-D cross-range FFT. The W-K algorithm rely on the use of Fast Fourier transforms (FFT), which may be computed very efficiently using this<sup>[7]</sup>. In the next step, matched filter finish bulk focusing that is to say the distance migration and imaging defocus result from the continuous motion of antenna array that can be compensated by multiplied by matched filter, the phase related with the matched filter is space-invariant, rely only on the range of scene center  $R_0$ , the frequency and cross-range wavenumber.

$$\begin{aligned} \Phi_{MF}(k_x, k_r, k_z) &= -2k_r R_0 + 2k_y R_0 \\ &= -2k_r R_0 + \sqrt{4k_r^2 - k_x^2 - k_z^2} R_0 \end{aligned} \quad (15)$$

After matched filter, by using the method of Stolt interpolation to compensated the residual distance migration and imaging defocus that can be implemented as 1-D interpolation change

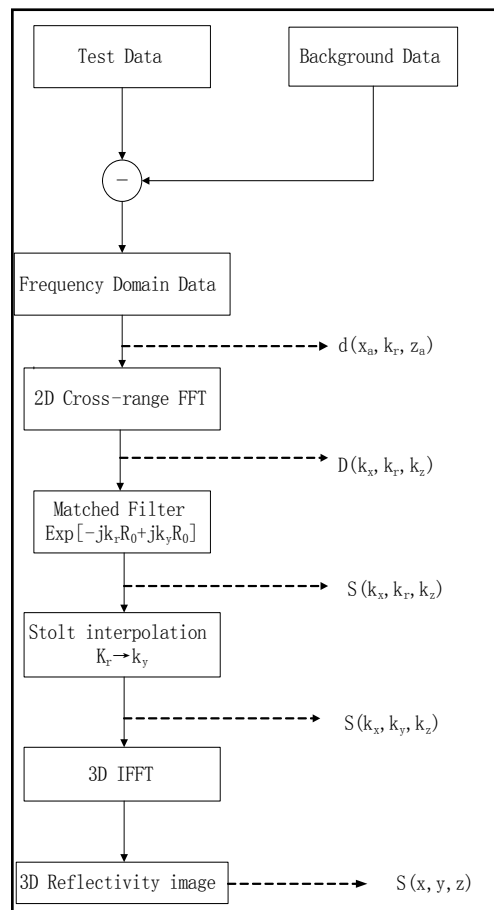


Fig. 2 : Block diagram of the 3-D RMA

variables  $(k_r \rightarrow k_y)$  could modify the amplitude term. The reflectivity image can be acquired by applying 3-D IFFT.

### III. Antenna Scan Interval And Imaging Space Resolution

The image-reconstruction technique discussed in the above sections depended on formation of three-dimensional imaging in the spatial

frequency domain. In the experiment, the scanning interval of antenna have to be chosen appropriately. When the scanning interval is oversize, the data of sample could not reconstruction. However, if the interval is undersize, there need more computation time which will make the imaging lose practicability<sup>[5]</sup>. So antenna scan interval  $\Delta x_a$ ,  $\Delta z_a$  and frequency interval  $\Delta f$  must abide by equation (16)-(18) in theory.

$$\Delta f \leq \frac{c}{2D_z} \tag{16}$$

$$\Delta x_a \leq \frac{\lambda_{\min} \sqrt{(L_x + D_x)^2 + (2R_0)^2}}{4(L_x + D_x)} \tag{17}$$

$$\Delta z_a \leq \frac{\lambda_{\min} \sqrt{(L_z + D_z)^2 + (2R_0)^2}}{4(L_z + D_z)} \tag{18}$$

Space resolution was decided by the equation (19), (20), (21), respectively. Millimeter-wave systems can be very high resolution due to the relatively short wavelength (1–10 mm)<sup>[9]</sup>. The resolution obtained in the image can be determined by experiment width of the coverage in the spacial frequency domain and the dimensions of the synthetic aperture.

$$\delta_x = \frac{\lambda_c R_0}{2L_x} \tag{19}$$

$$\delta_y = \frac{\lambda_c R_0}{2L_y} \tag{20}$$

$$\delta_z = \frac{c}{2B} \tag{21}$$

Where  $\lambda_{\min}$  is a min wavelength of the antenna;  $\lambda_c$  is the center of wavelength of the antenna ; B is the bandwidth of the antenna;  $L_x$ ,  $L_y$  is the range of space scan of the antenna, respectively(allows called aperture length);  $D_x, D_y, D_z$  is the range of target, but in fact the resolution can not reach the theory value.

**IV. Simulation Implementation and Result Analysis**

**A. Simulation result and analysis**

Through the theoretical analysis above, in this section, we will do the experiment. Single point target and multiple rectangle targets are acted as imaging target to simulation. The reference is selected in table 4.1.

Table 4.1 : imaging system of simulation reference

reference	numerical value
carrier frequency	37.5GHZ
bandwidth	5GHZ
Sample interval: $\Delta x_a$	0.005m
the number of antenna element	10000
sample interval: $\Delta z_a$	0.005m
The number of frequency samples (Nf)	200
reference distance (R0)	0.9m

The signal point target is described in Fig.3 which only select a

cross-section.

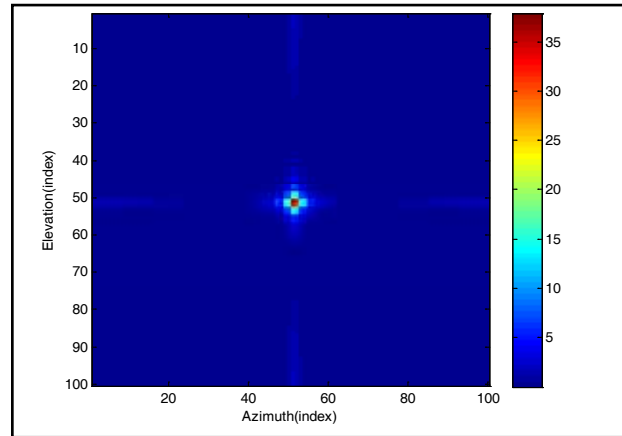


Fig. 3 : Simulation signal target imaging

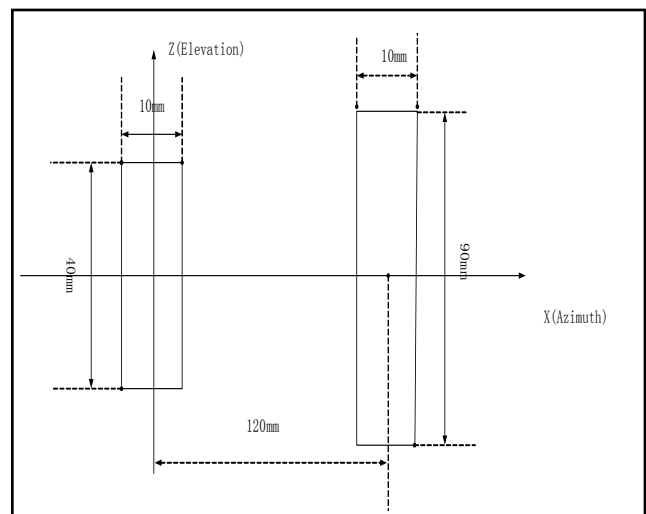


Fig. 4 : The experiment scene of model

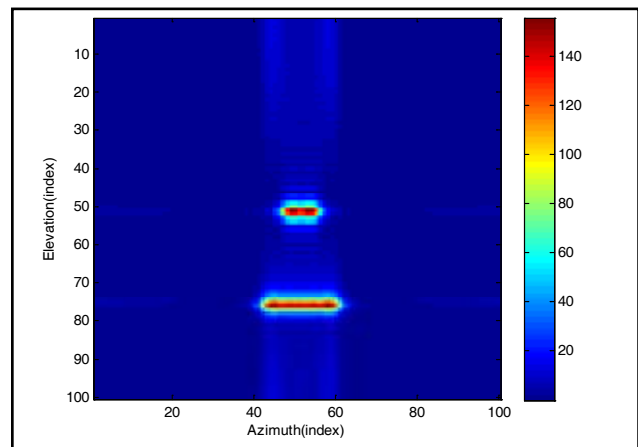


Fig. 5 : Simulation double rectangle area target imaging

Where azimuth is x direction, elevation is z direction. To prove the stability and effectiveness of 3-D RMA, the simulation of experiment scene is described in Fig.4 and then the multiple targets are reconstructed and the result are shown in Fig. 5. Their actual size are (0.04m,0.005m) (0.09m,0.005m) and simulation size are (0.05m,0.005m) (0.1m,0.005m) respectively. the precision is very high. So, the 3-D RMA is reliable and effective.

## B. Experiment result and analysis

Based on the introduction 3-D RMA in this paper, in order to verify the feasibility of this algorithm further, we dealt with the data of test. The reference coefficient the same as the simulation. Then the result of experiment system is shown in Fig.6.

We can see three-dimensional RMA imaging algorithm is much adapt to security checkpoints imaging. According to the imaging in figure 6 that is quite close to the actual model. And it only needs 4 minutes from the measured data of load to the imaging, so we can conclude that the proposed method is effective for security checkpoints imaging.

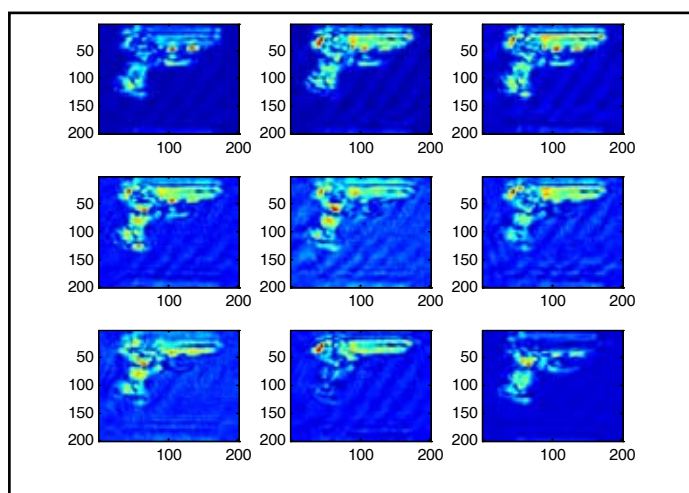


Fig. 6 : Actual measurement handgun imaging

## V. Conclusion

In the paper, 3-D RMA is proposed for security checkpoints imaging. The image reconstruction for this system uses near-field assumptions<sup>[7]</sup> and has theoretically nearly optimal resolution performance, in all three dimensions. The results on simulated and real datasets demonstrated the efficiency and feasibility of the millimeter-wave imaging technique. And the imaging time approximately reach 4 minutes. This procedure is performed by Matlab 7.1 codes in a Corell PC platform with a window 7 operation system, the PC has a dual-CPU running at 1.8GHz and a 2G bytes memory configure.

## VI. Acknowledgment

This work is supported by Scientific and Technological Research Program of Chongqing Municipal Education Commission (KJ130507).

## Reference

- [1] Sheen, D. M., D. L. McMakin, and T. E. Hall, "Three-dimensional millimeter-wave imaging for concealed weapon detection," *IEEE Trans. on Microwave Theory and Techniques*, Vol. 49, No. 9, 1581–1592, Sep. 2001.
- [2] S.Y. Li, B.L. Ren, H.J. Sun, W.D. Hu and X. Lv. Modified wavenumber domain algorithm for three-dimensional millimeter-wave imaging[J]. *Progress In Electromagnetics Research*, 2012, 124:35-53.
- [3] J. M. Lopez-Sanchez and J. Fortuny-Guasch, "3-D Radar imaging using range migration techniques," *IEEE Trans. Antennas Propagat.*, vol.48,pp. 728–737, May, 2000.
- [4] Joaquim Fortuny. Efficient algorithms for three-dimensional near-field synthetic aperture radar imaging[D]. Karlsruhe. Germany : Faculty of Electrical Engineering University of Karlsruhe, 2001.
- [5] 李亮, 苗俊刚, 江月松. 基于 Stolt 插值的近场三维雷达合成孔径成像[J]. *北京航空航天大学学报*, 2006,32(7) :815-818
- [5] L. Li, J.G.Mao, Y.S.Jiang. Based on the Stolt interpolation near-field three-dimensional synthetic aperture radar imaging[J]. *journal of beijing university of aeronautics and astronautics*, 2006,32(7) :815-816
- [6] Sheen, D. M., D. L. McMakin, H. D. Collins, T. E. Hall, and R. H. Severtsen, "Concealed explosive detection on personnel using a wideband holographic millimeter-wave imaging system," *Proceedings of SPIE*, Vol. 2755, 503–513, 1996.
- [7] Sheen, D., D. McMakin, and T. Hall, "Near-field three-dimensional radar imaging techniques and applications," *Applied Optics*, Vol. 49, E83–E93, Jun. 2010.
- [8] 任百玲, 主动毫米波安检成像算法及系统研究[D]. 北京: 北京理工大学, 2014.
- [8] B.L.Ren, *Research on Active Millimeter-Wave Imaging Algorithms and System for Security Inspection*[D]. Beijing:Beijing institute of technology, 2014.
- [9] W. X .Tan, "Study on theory and algorithms for three-dimensional synthetic aperture radar imaging," Ph.D. Thesis, Institute of Electronics, Chinese Academy of Sciences, 2009 (in Chinese).
- [10] K. K. Knaell and G. P. Cardillo, "Radar tomography for the generation of three-dimensional images," *Proc. Inst. Elect. Eng. Radar Sonar Navig.*, vol. 142, no. 2, pp. 54–60, 1995.